Available online at www.sciencedirect.com

ScienceDirect

Nuclear Physics B 938 (2019) 416–425

NUCLEAR PHYSICS B

www.elsevier.com/locate/nuclphysb

Coordinate space calculation of two- and three-loop sunrise-type diagrams, elliptic functions and truncated Bessel integral identities

S. Groote [a,*], J.G. Körner [b]

[a] *Füüsika Instituut, Tartu Ülikool, W. Ostwaldi 1, EE-50411 Tartu, Estonia*
[b] *Institut für Physik der Johannes-Gutenberg-Universität, Staudinger Weg 7, D-55099 Mainz, Germany*

Received 25 May 2018; received in revised form 26 November 2018; accepted 27 November 2018
Available online 29 November 2018
Editor: Stephan Stieberger

Abstract

We integrate three-loop sunrise-type vacuum diagrams in $D_0 = 4$ dimensions with four different masses using configuration space techniques. The finite parts of our results are in numerical agreement with corresponding three-loop calculations in momentum space. Using some of the closed form results of the momentum space calculation we arrive at new integral identities involving truncated integrals of products of Bessel functions. For the non-degenerate finite two-loop sunrise-type vacuum diagram in $D_0 = 2$ dimensions we make use of the known closed form p-space result to express the moment of a product of three Bessel functions in terms of a sum of Clausen polylogarithms. Using results for the nondegenerate two-loop sunrise diagram from the literature in $D_0 = 2$ dimensions we obtain a Bessel function integral identity in terms of elliptic functions.

1. Introduction

The computation of higher order vacuum diagrams in quantum field theory has been extended to ever higher loop levels involving different degrees of mass degeneracy and/or zero mass values

* Corresponding author.
E-mail address: groote@ut.ee (S. Groote).

https://doi.org/10.1016/j.nuclphysb.2018.11.023

for their mass configurations. The multi-loop calculations have traditionally been carried out in momentum space (p-space). For the sunrise-type subclass of these higher order vacuum diagrams it is much simpler to integrate the diagrams using configuration-space (x-space) techniques. The comparison of the results of the two calculations will provide a welcome nontrivial cross check on the correctness of the respective p- and x-space calculations in as much as a subclass of the vacuum diagrams are of sunrise-type. In addition, if one can avail of closed form p-space results, one arrives at new nontrivial integral identities involving moments of Bessel functions. In the case of the two-loop nondegenerate sunrise diagram this leads to an identity of moments of Bessel functions in terms of elliptic integrals. We mention that Bessel function integral identities involving elliptic functions have been studied before in Refs. [1,2].

This paper was triggered by the recent appearance of two p-space calculations of the non-degenerate three-loop vacuum diagrams (all four masses different). We numerically confirm the results of the vacuum sunrise-type diagrams in Refs. [3,4] using x-space techniques. In Sec. 2 we briefly review some general features of the x-space approach and describe the splitting technique used to separate singular (analytical) and finite (numerical) parts in $D = D_0 - 2\varepsilon$ spacetime dimensions where $D_0 = 4$ in the present application. The particular form of the splitting technique preserves the inherent symmetry of the nondegenerate multiloop vacuum and sunrise integrals w.r.t. the exchange of different rungs or masses in the diagrams. This leads to the notion of truncated Bessel integrals. In Sec. 3 we use closed form results for the finite parts of the three-loop vacuum diagrams from the literature to obtain new integral identities for a set of truncated Bessel integrals. In Sec. 4 we compare results for the nondegenerate two-loop sunrise diagram with results from Refs. [8–11] for $D_0 = 2$ to obtain again an integral identity. Our conclusions are given in Sec. 5, and series expansions for the Bessel functions are found in the Appendix.

2. Splitting technique for Bessel integrals

The configuration space calculation of n-loop sunrise-type diagrams with $N = n + 1$ different masses in arbitrary spacetime dimensions has been studied by us in a series of papers [12–19]. The starting point is the central identity for the p-space correlator function $\tilde{\Pi}(p; m_1, \ldots, m_{n+1})$ given by

$$\tilde{\Pi}(p; m_1, \ldots, m_{n+1}) = 2\pi^{\lambda+1} \int_0^\infty \left(\frac{px}{2}\right)^{-\lambda} J_\lambda(px) \prod_{i=1}^{n+1} D(x, m_i) x^{2\lambda+1} dx, \tag{1}$$

where $p = \sqrt{p^2}$ and $x = \sqrt{x^2}$ are the absolute values of the four-vectors of four-momentum and spacetime, respectively. The relation of the spacetime dimension to the parameter λ is given by $D = 2\lambda + 2$. n-loop sunrise-type integrals are UV divergent for $nD \geq 2(n + 1)$ (or $n\lambda > 1$). In order to parametrize the singularities, we use dimensional regularization by choosing $D = D_0 - 2\varepsilon$. $J_\lambda(z)$ is the Bessel function of the first kind, and

$$D(x, m) = \int \frac{d^D p}{(2\pi)^D} \frac{e^{ip_\mu x^\mu}}{p^2 + m^2} = \frac{(mx)^\lambda K_\lambda(mx)}{(2\pi)^{\lambda+1} x^{2\lambda}} \tag{2}$$

is the free propagator in (Euclidean) spacetime for a particle line with mass m. The function $K_\lambda(mx)$ denotes the Bessel function of the second kind, also known as the McDonald function. The series expansions for both Bessel functions are found in the Appendix. In the case that the particle mass vanishes ($m = 0$), the propagator simplifies to

$$D(x,0) = \int \frac{d^D p}{(2\pi)^D} \frac{e^{ip_\mu x^\mu}}{p^2} = \frac{\Gamma(\lambda)}{4\pi^{\lambda+1} x^{2\lambda}}, \tag{3}$$

since the corresponding Bessel function of the second kind is replaced by a simple power dependence. A corresponding simplification occurs in the case of a vacuum diagram ($p^2 \to 0$) where one has

$$\left(\frac{px}{2}\right)^{-\lambda} J_\lambda(px) \to \frac{1}{\Gamma(\lambda+1)}. \tag{4}$$

Additional features can easily be implemented in the configuration space calculus. For instance, higher powers of propagators can be inserted by calculating the derivative with respect to the corresponding squared mass, i.e.

$$\tilde{D}^{(\kappa)}(p,m) = \frac{1}{(p^2+m^2)^{\kappa+1}} = \frac{1}{\Gamma(\kappa+1)} \left(\frac{-\partial}{\partial m^2}\right)^\kappa \frac{1}{p^2+m^2} \tag{5}$$

which leads to

$$D^{(\kappa)}(x,m) = \int \frac{d^D p}{(2\pi)^D} \frac{e^{ip_\mu x^\mu}}{(p^2+m^2)^{\kappa+1}} = \frac{(m/x)^{\lambda-\kappa}}{(2\pi)^{\lambda+1} 2^\kappa \Gamma(\kappa+1)} K_{\lambda-\kappa}(mx). \tag{6}$$

Bessel integral identities involving up to three Bessel functions have been compiled in integral tables (cf. for instance Refs. [20,21]). Some Bessel function integrals involving up to six Bessel functions can be found in Refs. [1,2]. To proceed one needs analytical expressions for the singular part of the result. However, this problem can be circumvented because in certain kinematical cases (small momentum or specific mass configurations) one can expand the Bessel functions in Taylor series to obtain a series expansion of the Bessel integral. In Ref. [18] we explained how the Bessel integral can be calculated by expanding the Bessel function of the first kind or, in case of vacuum diagrams, one or more McDonald functions.[1] However, in such an expansion the symmetry with respect to the exchanges of the different masses in the diagram is no longer manifest.

In order to avoid this problem, we use another approach to isolate the divergent parts of the integrals. Namely, we use the Gaussian factor $e^{-\mu^2 x^2}$ to protect the integrand against the divergent upper limit. The mass parameter μ in the exponent defines a new regularization scale parameter. In detail, we add and subtract a series expansion of the product of Bessel functions multiplied by $e^{\mu^2 x^2}$ to a specified order. The order of the series expansion is chosen such that the difference is no longer singular at $x = 0$. The series can be integrated analytically using

$$\int_0^\infty x^{p-1} e^{-\mu^2 x^2} dx = \frac{1}{2} \mu^{-p} \Gamma(p/2) \tag{7}$$

where the r.h.s. can be expanded in ε. The integral

$$\int_0^\infty [f(x)]_x dx \tag{8}$$

[1] In this approach, at least one single McDonald function has to stay unexpanded to guarantee the convergence of the integrand for large values of x.

will be called truncated integral in the following. The truncated integral involves a series truncation

$$[f(x)]_x := f(x) - e^{-\mu^2 x^2}\left(e^{\mu^2 x^2} f(x) + O(x)\right), \tag{9}$$

where $f(x)$ is the original integrand in Eq. (1). The difference is integrable numerically even in the limit $\varepsilon \to 0$ and constitutes a part of the finite contribution. Of course, the regularized integral depends on the (arbitrary) mass scale μ. However, taking into account the integrated series expansion leading to a power series in inverse powers of ε, the scale dependence cancels out, as it should be according to the construction.

With the techniques described in this section we have recalculated the nondegenerate three-loop sunrise-type vacuum diagrams in Refs. [3,4] and have checked our results against the results given in Refs. [3,4]. For the relations

$$\begin{aligned}
\tilde{\Pi}(0; m_1, m_2, m_3, m_4) &= -\frac{e^{-3\gamma_E \varepsilon}}{4^{6-3\varepsilon}} M(1,1,1,1,0,0; m_1^2, m_2^2, m_3^2, m_4^2, 0, 0),\\
\tilde{\Pi}(0; \dot{m}_1, m_2, m_3, m_4) &= -\frac{e^{-3\gamma_E \varepsilon}}{4^{6-3\varepsilon}} M(2,1,1,1,0,0; m_1^2, m_2^2, m_3^2, m_4^2, 0, 0)
\end{aligned} \tag{10}$$

(cf. Ref. [3], a dot at the mass entry in $\tilde{\Pi}$ indicates the multiplicity) and

$$\begin{aligned}
\tilde{\Pi}(0; m_1, m_2, m_3, m_4) &= \frac{e^{-3\gamma_E \varepsilon}}{(4\pi)^{6-3\varepsilon}} \mathbf{E}(m_1^2, m_2^2, m_3^2, m_4^2),\\
\tilde{\Pi}(0; \dot{m}_1, m_2, m_3, m_4) &= \frac{e^{-3\gamma_E \varepsilon}}{(4\pi)^{6-3\varepsilon}} \mathbf{F}(m_1^2, m_2^2, m_3^2, m_4^2)
\end{aligned} \tag{11}$$

(cf. possible mass constellations in Ref. [4]) we have found numerical agreement. In case of Ref. [3], this comparison was performed with the help of the code TVID [22] for randomly generated sets of four different masses in a total sample of 1000 mass configurations.

For the genuine sunrise diagram, a comparison is possible also to results with equal [5] and different masses [6] expressed in terms of multiple elliptic polylogarithms [7].

3. Truncated Bessel integrals for $D_0 = 4$

For some sunrise-type diagrams, p-space calculations have led to analytic closed form results. These results can be used as input to derive Bessel function integral identities by comparison with the corresponding x-space results. As emphasized before, sunrise-type diagrams in $D_0 = 4$ dimensions have to be regularized, implying that the corresponding integral identities have to be formulated in terms of truncated Bessel integrals. A complete list of analytical results for vacuum diagrams of sunrise-type topology known up to three-loop order is given in Ref. [4]. We have used the analytical results for $\mathbf{E}(u, v, y, z)$ (corresponding to Fig. 1(a)) and $\mathbf{F}(u, v, y, z)$ (corresponding to Fig. 1(b)) given in Ref. [4] to calculate truncated Bessel integrals. By choosing $\mu = 1$ we obtain

$$\int_0^\infty \left[\frac{32 a K_1(ax)}{x^4}\right]_x dx \;=\; 4 - \frac{17}{8}a^4 + \frac{1}{2}a^2(16 + 5a^2)\ell_a - a^4\ell_a^2 - \frac{1}{8}a^4\pi^2,$$

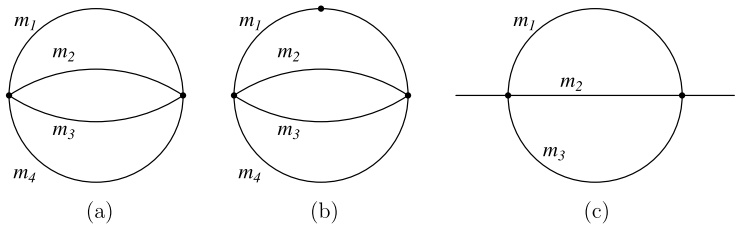

Fig. 1. Three-loop nondegenerate vacuum diagrams (a) without and (b) with a derivative indicated by a dot on the top line. Diagram (c) shows a two-loop (genuine) sunrise diagram with three different masses.

$$\int_0^\infty \left[\frac{32a^2K_1(ax)^2}{x^3}\right]_x dx = 4 - \frac{19}{4}a^4 + a^2(16+3a^2)\ell_a + 2a^4\ell_a^2 - \frac{8}{3}a^4\ell_a^3 + \frac{1}{12}a^4\pi^2 - \frac{1}{3}a^4\pi^2\ell_a + \frac{10}{3}a^4\zeta(3),$$

$$\int_0^\infty \left[\frac{32a^3K_1(ax)^3}{x^2}\right]_x dx = 4 - \frac{63}{8}a^4 + \frac{3}{2}a^2(16+a^2)\ell_a + 9a^4\ell_a^2 - 8a^4\ell_a^3 - \frac{5}{8}a^4\pi^2 - a^4\pi^2\ell_a + \frac{3}{2}a^4\psi'\left(\frac{1}{3}\right) + 2a^4\zeta(3),$$

$$\int_0^\infty \left[\frac{32a^4K_1(ax)^4}{x}\right]_x dx = 4 - \frac{23}{2}a^4 + 2a^2(16-a^2)\ell_a + 20a^4\ell_a^2 - 16a^4\ell_a^3 + \frac{5}{6}a^4\pi^2 - 2a^4\pi^2\ell_a + 4a^4\zeta(3),$$

$$\begin{aligned}\int_0^\infty \left[\frac{32abK_1(ax)K_1(bx)}{x^3}\right]_x dx &= 4 - \frac{1}{2}a^2b^2 - \frac{17}{8}(a^2+b^2) - \frac{1}{24}(a^4-4a^2b^2+b^4)\pi^2 \\ &+ \frac{a^2}{2}(16+5a^2-2b^2)\ell_a + \frac{b^2}{2}(16-2a^2+5b^2)\ell_b - \frac{1}{6}a^2b^2\pi^2(\ell_a+\ell_b) \\ &- \frac{1}{2}(a^4-b^4)\ell_a^2 - (a^4-4a^2b^2+b^4)\ell_a\ell_b + \frac{1}{2}(a^4-b^4)\ell_b^2 \\ &+ \frac{2}{3}a^2b^2\ell_a^3 - 2a^2b^2\ell_a^2\ell_b - 2a^2b^2\ell_a\ell_b^2 + \frac{2}{3}a^2b^2\ell_b^3 + \frac{4}{3}a^2b^2\zeta(3) \\ &+ \frac{1}{4}(a^4-b^4)\left[\mathrm{Li}_2\left(1-\frac{a^2}{b^2}\right) - \mathrm{Li}_2\left(1-\frac{b^2}{a^2}\right)\right] \\ &+ a^2b^2\left[\mathrm{Li}_3\left(\frac{a^2}{b^2}\right) + \mathrm{Li}_3\left(\frac{b^2}{a^2}\right) - \frac{1}{2}\ln\left(\frac{a^2}{b^2}\right)\left\{\mathrm{Li}_2\left(\frac{a^2}{b^2}\right) - \mathrm{Li}_2\left(\frac{b^2}{a^2}\right)\right\}\right],\end{aligned}$$

$$\begin{aligned}\int_0^\infty \left[\frac{32a^2b^2K_1(ax)^2K_1(bx)^2}{x}\right]_x dx &= 4 - 2a^2b^2 - \frac{19}{4}(a^4+b^4) \\ &+ \frac{1}{12}(a^4+8a^2b^2+b^4)\pi^2 + a^2(16+3a^2-4b^2)\ell_a + b^2(16-4a^2+3b^2)\ell_b\end{aligned}$$

$$
\begin{aligned}
&- \frac{a^2}{3}(a^2+2b^2)\pi^2\ell_a - \frac{b^2}{3}(2a^2+b^2)\pi^2\ell_b + 2a^2(a^2-2b^2)\ell_a^2 \\
&+ 24a^2b^2\ell_a\ell_b - 2b^2(2a^2-b^2)\ell_b^2 + \frac{2}{3}(5a^4-4a^2b^2+5b^4)\zeta(3) \\
&- \frac{4}{3}(a^2-b^2)^2\ell_a^3 - 4(a^4+2a^2b^2-b^4)\ell_a^2\ell_b + 4(a^4-2a^2b^2-b^4)\ell_a\ell_b^2 \\
&- \frac{4}{3}(a^2-b^2)^2\ell_b^3 + (a^2-b^2)^2\Bigg[\mathrm{Li}_3\left(\frac{a^2}{b^2}\right) + \mathrm{Li}_3\left(\frac{b^2}{a^2}\right) \\
&\quad - \frac{1}{2}\ln\left(\frac{a^2}{b^2}\right)\left\{\mathrm{Li}_2\left(\frac{a^2}{b^2}\right) - \mathrm{Li}_2\left(1-\frac{a^2}{b^2}\right) - \mathrm{Li}_2\left(\frac{b^2}{a^2}\right) + \mathrm{Li}_2\left(1-\frac{b^2}{a^2}\right)\right\}\Bigg], \\
&\int_0^\infty \left[\frac{32ab^2K_1(ax)K_1(bx)^2}{x^2}\right]_x dx \;=\; 4 - a^2b^2 - \frac{1}{8}(17a^4+38b^4) \\
&- \frac{1}{24}(a^4-8a^2b^2-2b^4)\pi^2 + \frac{1}{2}a^2(16+5a^2-4b^2)\ell_a + b^2(16-2a^2+3b^2)\ell_b \\
&- \frac{1}{3}a^2b^2\pi^2\ell_a - \frac{1}{3}b^2(a^2+b^2)\pi^2\ell_b - 2a^2(a^2-4b^2)\ell_a\ell_b + (a^4+2b^4)\ell_b^2 \\
&- 8a^2b^2\ell_a\ell_b^2 + \frac{8}{3}b^2(a^2-b^2)\ell_b^3 + \frac{2}{3}b^2(4a^2-b^2)\zeta(3) \\
&- \frac{a}{2}(a^2+2b^2)\sqrt{a^2-4b^2}\left[\mathrm{Li}_2\left(-\frac{a-\sqrt{a^2-4b^2}}{a+\sqrt{a^2-4b^2}}\right) - \mathrm{Li}_2\left(-\frac{a+\sqrt{a^2-4b^2}}{a-\sqrt{a^2-4b^2}}\right)\right] \\
&- 2b^2(a^2-b^2)\left[\mathrm{Li}_3\left(-\frac{a-\sqrt{a^2-4b^2}}{a+\sqrt{a^2-4b^2}}\right) + \mathrm{Li}_3\left(-\frac{a+\sqrt{a^2-4b^2}}{a-\sqrt{a^2-4b^2}}\right)\right], \qquad (12)
\end{aligned}
$$

where

$$
\ell_a := \ln\left(\frac{a}{2}\right) + \frac{1}{2}\gamma_E, \qquad \ell_b := \ln\left(\frac{b}{2}\right) + \frac{1}{2}\gamma_E. \qquad (13)
$$

The parameters a and b are mass parameters associated with the vacuum diagrams. All seven of these truncated Bessel function integral identities have been checked numerically using MATHEMATICA.

4. Bessel integrals and elliptic functions for $D_0 = 2$

It is well known that the correlator function $\tilde{\Pi}(p; m_1, \ldots, m_{n+1})$ for the sunrise-type diagrams is finite in $D_0 = 2$ dimensions. Therefore, the corresponding Bessel integrals need not be truncated.

For the vacuum integrals ($p^2 = 0$) the comparison with results from Refs. [23–26] results in

$$
\int_0^\infty 2xK_0(m_1x)K_0(m_2x)K_0(m_3x)dx = \frac{1}{\sqrt{-\lambda}}\left(\mathrm{Cl}_2(\alpha_1) + \mathrm{Cl}_2(\alpha_2) + \mathrm{Cl}_2(\alpha_3)\right), \qquad (14)
$$

where $\lambda = \lambda(m_1^2, m_2^2, m_3^2) = m_1^4 + m_2^4 + m_3^4 - 2m_1^2m_2^2 - 2m_1^2m_3^2 - 2m_2^2m_3^2$ is the Källén function, and $\mathrm{Cl}_p(z)$ is the Clausen polylogarithm,

$$\mathrm{Cl}_p(\alpha) := \frac{1}{2i}\left(\mathrm{Li}_p(e^{i\alpha}) - \mathrm{Li}_p(e^{-i\alpha})\right) \tag{15}$$

with arguments $\alpha_i = 2\arctan(\sqrt{-\lambda}/\delta_i)$, where

$$\delta_1 = -m_1^2 + m_2^2 + m_3^2, \qquad \delta_2 = m_1^2 - m_2^2 + m_3^2, \qquad \delta_3 = m_1^2 + m_2^2 - m_3^2. \tag{16}$$

For the more general case $p^2 \neq 0$ (cf. Fig. 1(c)), analytical results have been given in Refs. [8, 9] in terms of elliptic polylogarithms

$$\mathrm{ELi}_{m;n}(x;y;z) = \sum_{j=1}^{\infty}\sum_{k=1}^{\infty}\frac{x^j}{j^m}\frac{y^k}{k^n}z^{jk}. \tag{17}$$

In order to understand the construction, we start with the complete elliptic integral

$$K(k) = \int_0^1 \frac{dt}{\sqrt{(1-t^2)(1-k^2t^2)}} \tag{18}$$

for the arguments

$$k_\pm := \sqrt{\frac{1}{2} \pm \frac{p^4 + 2(m_1^2+m_2^2+m_3^2)p^2 + \lambda(m_1^2,m_2^2,m_3^2)}{2\sqrt{(p^2+\mu_1^2)(p^2+\mu_2^2)(p^2+\mu_3^2)(p^2+\mu_4^2)}}}, \tag{19}$$

where μ_i are the (pseudo)thresholds

$$\begin{aligned}
\mu_1 &= m_1 + m_2 - m_3,\\
\mu_2 &= m_1 - m_2 + m_3,\\
\mu_3 &= -m_1 + m_2 + m_3,\\
\mu_4 &= m_1 + m_2 + m_3.
\end{aligned} \tag{20}$$

While the second argument of the elliptic polylogarithm is -1, the last argument is given by $-q$ where

$$q = \exp\left(-\pi\frac{K(k_+)}{K(k_-)}\right). \tag{21}$$

Defining a modified Clausen dilogarithm by

$$\tilde{\mathrm{Cl}}_2(\tilde{\alpha}) := \frac{1}{2i}\left(\mathrm{Li}_2(e^{i\tilde{\alpha}}) - \mathrm{Li}_2(e^{-i\tilde{\alpha}}) + 2\,\mathrm{ELi}_{2;0}(e^{i\tilde{\alpha}};-1;-q) - 2\,\mathrm{ELi}_{2;0}(e^{-i\tilde{\alpha}};-1;-q)\right), \tag{22}$$

the comparison gives

$$\begin{aligned}
&\int_0^\infty 2x\,J_0(px)K_0(m_1x)K_0(m_2x)K_0(m_3x)dx\\
&\quad = \frac{2K(k_+)\left(\tilde{\mathrm{Cl}}_2(\tilde{\alpha}_1) + \tilde{\mathrm{Cl}}_2(\tilde{\alpha}_2) + \tilde{\mathrm{Cl}}_2(\tilde{\alpha}_3)\right)}{\sqrt[4]{(p^2+\mu_1^2)(p^2+\mu_2^2)(p^2+\mu_3^2)(p^2+\mu_4^2)}\,\pi},
\end{aligned} \tag{23}$$

where

$$\tilde{\alpha}_i = \pi \frac{F(k_i^{-1}, k_+)}{K(k_+)}, \qquad k_i = \sqrt{k_+^2 + \frac{4m_j^2 m_k^2}{\sqrt{(p^2+\mu_1^2)(p^2+\mu_2^2)(p^2+\mu_3^2)(p^2+\mu_4^2)}}} \tag{24}$$

((i, j, k) is a cyclic permutation of $(1, 2, 3)$) and the incomplete elliptic integral is given by

$$F(t_0, k) := \int_0^{t_0} \frac{dt}{\sqrt{(1-t^2)(1-k^2t^2)}}. \tag{25}$$

The result (23) holds only for the component of the Riemann sheet connected to the equal mass case $m_1 = m_2 = m_3$. Problems for other mass configurations with Eq. (23) can be revealed already in the limit $p^2 \to 0$. Obviously, in his limit the main square root simplifies to

$$\sqrt{(p^2+\mu_1^2)(p^2+\mu_2^2)(p^2+\mu_3^2)(p^2+\mu_4^2)} \to -\lambda. \tag{26}$$

Further, one has $k_- = 1$ and $k_+ = 0$. Thus $q \to 0$, and the elliptic polylogarithms vanish. However, for the arguments of the (modified) Clausen dilogarithms one obtains

$$\tilde{\alpha}_i = 2 \arcsin\left(\sqrt{\frac{-\lambda}{4m_j^2 m_k^2}}\right) \quad \Leftrightarrow \quad \frac{-\lambda}{4m_j^2 m_k^2} = \sin^2\left(\frac{\tilde{\alpha}_i}{2}\right), \tag{27}$$

leading to

$$\tan\left(\frac{\tilde{\alpha}_i}{2}\right) = \frac{\sqrt{-\lambda}}{\sqrt{\delta_i^2}} \quad \Leftrightarrow \quad \tilde{\alpha}_i = 2 \arctan\left(\frac{\sqrt{-\lambda}}{\sqrt{\delta_i^2}}\right). \tag{28}$$

Only in the case $\delta_i > 0$ $(i = 1, 2, 3)$ and if one is close to the equal mass case, one can reconstruct the α_i. As mentioned in Ref. [27], the problem is caused by the standard convention for mathematical software which is in conflict with the Feynman prescription used in quantum field theory. In Ref. [28] the region in the projective plane restricted by $\lambda(m_1^2, m_2^2, m_3^2) < 0$ is called the Källén triangle. In terms of Ref. [28] the restriction $\delta_i > 0$ $(i = 1, 2, 3)$ leads to a region enclosed by the three circles of the projective plane about the three corners through the midpoints of the edges, deforming the Källén triangle to a hyperbolic triangle.[2] We emphasize that our configuration space method is free from such kind of problems and, therefore, can be used to check existing analytical results in these problematic cases.

5. Summary and conclusions

We have recalculated nondegenerate sunrise-type three-loop vacuum integrals in x-space and have found numerical agreement with corresponding results obtained by p-space calculations. The agreement of the respective results can be considered to be a necessary – but not sufficient – check on the rather involved p-space three-loop vacuum diagram calculations. It is not difficult to

[2] Because of a definition of projectivity in squared masses instead of a definition in linear masses, the "Källén triangle" is deformed to a circle in Ref. [29], while the region $\delta_i > 0$ would be given by a triangle.

extend the x-space calculation of the sunrise-type vacuum diagrams to higher loop orders where they can again be used to check on the results of higher loop vacuum diagram calculations in p-space when they become available in the future. In fact, the authors of Ref. [30] have checked their p-space results on the degenerate (all masses equal) five-loop sunrise-type vacuum integrals against the x-space results of e.g. Ref. [18].

By comparing the results of some p-space and x-space calculations of specific two- and three-loop sunrise diagrams we have presented a number of novel Bessel function integral identities that would be difficult to prove otherwise. For divergent sunrise integrals we have introduced a regularization procedure in terms of a truncation which lead to a number of novel truncated Bessel function integral identities. For the nondegenerate genuine two-loop sunrise diagram in two dimensions we have obtained, again by comparing x- and p-space results, a Bessel function integral identity in terms of elliptic functions. It appears that the techniques discussed in this paper can open a Pandora's box of new Bessel function integral identities.

Acknowledgements

We would like to thank A. Freitas for very constructive e-mail exchanges on the mutual numerical evaluation of the vacuum integrals. This research was supported by the Estonian Research Council under Grant No. IUT2-27. S.G. acknowledges the support of the theory group THEP at the Institute of Physics and of the Cluster of Excellence PRISMA at the University of Mainz.

Appendix A. Series expansions of the Bessel functions

The two Bessel functions $J_\lambda(z)$ and $K_\lambda(z)$ used in this paper are defined via the following Taylor series expansions,

$$\begin{aligned} J_\lambda(z) &= \left(\frac{z}{2}\right)^\lambda \sum_{k=0}^{\infty} \frac{(-z^2/4)^k}{k!\Gamma(\lambda+k+1)} \\ &= \frac{(z/2)^\lambda}{\Gamma(1+\lambda)}\left(1 - \frac{(z/2)^2}{(1+\lambda)} + \frac{(z/2)^4}{2(1+\lambda)(2+\lambda)} - \frac{(z/2)^6}{6(1+\lambda)(2+\lambda)(3+\lambda)} + O(z^8)\right), \end{aligned} \tag{A.1}$$

$$\begin{aligned} K_\lambda(z) &= \frac{\pi}{2\sin(\lambda\pi)}\left(I_{-\lambda}(z) - I_\lambda(z)\right) = \frac{1}{2}\Gamma(\lambda)\Gamma(1-\lambda)\left(I_{-\lambda}(z) - I_\lambda(z)\right) \\ &= \frac{1}{2}\Gamma(\lambda)\Gamma(1-\lambda)\left(\frac{(z/2)^{-\lambda}}{\Gamma(1-\lambda)}\left(1 + \frac{(z/2)^2}{1-\lambda} + \ldots\right) - \frac{(z/2)^\lambda}{\Gamma(1+\lambda)}\left(1 + \frac{(z/2)^2}{1+\lambda} + \ldots\right)\right) \\ &= \frac{1}{2}\Gamma(\lambda)\left(\frac{z}{2}\right)^{-\lambda}\left(1 + \frac{(z/2)^2}{(1-\lambda)} + \ldots\right) + \frac{1}{2}\Gamma(-\lambda)\left(\frac{z}{2}\right)^{\lambda}\left(1 + \frac{(z/2)^2}{(1+\lambda)} + \ldots\right), \end{aligned} \tag{A.2}$$

where we have used

$$\begin{aligned} I_\lambda(z) &= \left(\frac{z}{2}\right)^\lambda \sum_{k=0}^{\infty} \frac{(z^2/4)^k}{k!\Gamma(\lambda+k+1)} \\ &= \frac{(z/2)^\lambda}{\Gamma(1+\lambda)}\left(1 + \frac{(z/2)^2}{(1+\lambda)} + \frac{(z/2)^4}{2(1+\lambda)(2+\lambda)} + \frac{(z/2)^6}{6(1+\lambda)(2+\lambda)(3+\lambda)} + O(z^8)\right). \end{aligned} \tag{A.3}$$

References

[1] D.H. Bailey, J.M. Borwein, D. Broadhurst, M.L. Glasser, Elliptic integral evaluations of Bessel moments, J. Phys. A 41 (2008) 205203.
[2] D. Broadhurst, Elliptic integral evaluation of a Bessel moment by contour integration of a lattice Green function, arXiv:0801.4813 [hep-th].
[3] A. Freitas, Three-loop vacuum integrals with arbitrary masses, J. High Energy Phys. 1611 (2016) 145.
[4] S.P. Martin, D.G. Robertson, Evaluation of the general 3-loop vacuum Feynman integral, Phys. Rev. D 95 (2017) 016008.
[5] S. Bloch, P. Vanhove, The elliptic dilogarithm for the sunset graph, J. Number Theory 148 (2015) 328.
[6] J. Broedel, C. Duhr, F. Dulat, L. Tancredi, Elliptic polylogarithms and iterated integrals on elliptic curves II: an application to the sunrise integral, Phys. Rev. D 97 (2018) 116009.
[7] Francis C.S. Brown, Andrey Levin, Multiple elliptic polylogarithms, arXiv:1110.6917 [math.NT].
[8] L. Adams, C. Bogner, S. Weinzierl, The two-loop sunrise graph in two space–time dimensions with arbitrary masses in terms of elliptic dilogarithms, J. Math. Phys. 55 (2014) 102301.
[9] L. Adams, C. Bogner, S. Weinzierl, The sunrise integral around two and four space–time dimensions in terms of elliptic polylogarithms, Acta Phys. Pol. B 46 (2015) 2131.
[10] E. Remiddi, L. Tancredi, Differential equations and dispersion relations for Feynman amplitudes. The two-loop massive sunrise and the kite integral, Nucl. Phys. B 907 (2016) 400.
[11] A. Primo, L. Tancredi, Maximal cuts and differential equations for Feynman integrals. An application to the three-loop massive banana graph, Nucl. Phys. B 921 (2017) 316.
[12] S. Groote, J.G. Körner, A.A. Pivovarov, A new technique for computing the spectral density of sunset type diagrams: integral transformation in configuration space, Phys. Lett. B 443 (1998) 269.
[13] S. Groote, J.G. Körner, A.A. Pivovarov, On the evaluation of sunset-type Feynman diagrams, Nucl. Phys. B 542 (1999) 515.
[14] S. Groote, J.G. Körner, A.A. Pivovarov, Configuration space based recurrence relations for sunset-type diagrams, Eur. Phys. J. C 11 (1999) 279.
[15] S. Groote, J.G. Körner, A.A. Pivovarov, Transcendental numbers and the topology of three loop bubbles, Phys. Rev. D 60 (1999) 061701.
[16] S. Groote, A.A. Pivovarov, Threshold expansion of Feynman diagrams within a configuration space technique, Nucl. Phys. B 580 (2000) 459.
[17] S. Groote, J.G. Körner, A.A. Pivovarov, Laurent series expansion of sunrise type diagrams using configuration space techniques, Eur. Phys. J. C 36 (2004) 471.
[18] S. Groote, J.G. Körner, A.A. Pivovarov, On the evaluation of a certain class of Feynman diagrams in x-space: sunrise-type topologies at any loop order, Ann. Phys. 322 (2007) 2374.
[19] S. Groote, J.G. Körner, A.A. Pivovarov, A numerical test of differential equations for one- and two-loop sunrise diagrams using configuration space techniques, Eur. Phys. J. C 72 (2012) 2085.
[20] A.P. Prudnikov, Yu.A. Brychkov, O.I. Marichev, Integrals and Series, vol. 2, Gordon and Breach, New York, 1990.
[21] I.S. Gradshteyn, I.M. Ryzhik, Tables of Integrals, Series, and Products, Academic Press, 1994.
[22] S. Bauberger, A. Freitas, TVID: Three-loop Vacuum Integrals from Dispersion relations, arXiv:1702.02996 [hep-ph].
[23] N.I. Usyukina, A.I. Davydychev, An approach to the evaluation of three and four point ladder diagrams, Phys. Lett. B 298 (1993) 363.
[24] H.J. Lu, C.A. Perez, Massless one loop scalar three point integral and associated Clausen, Glaisher and L functions, SLAC-PUB-5809.
[25] Z. Bern, L.J. Dixon, D.A. Kosower, S. Weinzierl, One loop amplitudes for $e^+e^- \to \bar{q}q\bar{Q}Q$, Nucl. Phys. B 489 (1997) 3.
[26] L. Adams, C. Bogner, S. Weinzierl, The two-loop sunrise graph with arbitrary masses, J. Math. Phys. 54 (2013) 052303.
[27] C. Bogner, A. Schweitzer, S. Weinzierl, Analytic continuation and numerical evaluation of the kite integral and the equal mass sunrise integral, Nucl. Phys. B 922 (2017) 528.
[28] L. Kaldamäe, S. Groote, Virtual and real processes, the Källén function, and the relation to dilogarithms, J. Phys. G 42 (2015) 085003.
[29] P. Burda, B. Kol, R. Shir, Vacuum seagull: evaluating a three-loop Feynman diagram with three mass scales, Phys. Rev. D 96 (2017) 125013.
[30] T. Luthe, Y. Schröder, J. Phys. Conf. Ser. 762 (2016) 012066.